Nanomedicine and Nanotoxicology

Surender Kumar Sharma
Hamed Nosrati
Taras Kavetskyy *Editors*

Harnessing Materials for X-ray Based Cancer Therapy and Imaging

Springer

Nanomedicine and Nanotoxicology

Series Editor

V. Zucolotto, Institute of Physics São Carlos, University of São Paulo,
São Carlos, São Paulo, Brazil

"Nanomedicine and Nanotoxicology" is a book Series dedicated to the application of Nanotechnology to achieve breakthroughs in healthcare as well as its risks and impact on the human body and environment. This book Series welcomes manuscripts on in vivo and in vitro diagnostics to therapy including targeted delivery, magnetic resonance imaging (MRI) and regenerative medicine; interface between nanomaterials (surfaces, particles, etc.) or analytical instruments with living human material (cells, tissue, body fluids); new tools and methods that impact significantly existing conservative practices; nanoparticles interaction with biological systems, and their risk assessments; among others. To submit a proposal or request further information, please contact Dr. Mayra Castro, Editor Applied Sciences, via mayra.castro@springer.com

More information about this series at https://link.springer.com/bookseries/10620

Surender Kumar Sharma · Hamed Nosrati ·
Taras Kavetskyy
Editors

Harnessing Materials for X-ray Based Cancer Therapy and Imaging

Springer

Editors
Surender Kumar Sharma
Central University of Punjab
Bathinda, India

Taras Kavetskyy
John Paul II Catholic University of Lublin
Lublin, Poland

Hamed Nosrati
Zanjan Pharmaceutical Biotechnology
Research Center
Zanjan University of Medical Sciences
Zanjan, Iran

ISSN 2194-0452 ISSN 2194-0460 (electronic)
Nanomedicine and Nanotoxicology
ISBN 978-3-031-04070-2 ISBN 978-3-031-04071-9 (eBook)
https://doi.org/10.1007/978-3-031-04071-9

This Springer imprint is published by the registered company Springer Nature Switzerland AG
The registered company address is: Gewerbestrasse 11, 6330 Cham, Switzerland

Contents

X-rays Based Bioimaging Techniques and Scintillating Materials

Gopal Niraula, Jason J. A. Medrano, Mohan C. Mathpal, Jero-R Maze, Jose A. H. Coaquira, and Surender K. Sharma

Abstract X-ray scintillators are broadly connected in cancer radiotherapy, warm treatment, and clinical diagnosis as therapeutic imaging materials since of their astonishing penetration control in tissues and organs. These X-ray energized scintillators can be focused on in cancer-site which retain and change over X-rays into unmistakable light outflows and diminishes the chance of overdose X-ray presentation to the typical cells. A few X-ray-based strategies have been illustrated for non-invasive high-resolution imaging of thick natural examples. These methods are undertaking to enhance our understanding and in situ natural chemistry and illness pathology examinations. In this chapter, we show those X-ray-based procedures and as of late outlined X-ray energized scintillators to offer an outline of such materials for the therapeutic diagnosis, imaging, and treatment.

G. Niraula · S. K. Sharma (✉)
Department of Physics, Federal University of Maranhao, Sao Luis, MA 65080-805, Brazil
e-mail: surender.sharma@ufma.br; surender.sharma@cup.edu.in

G. Niraula · J. A. H. Coaquira
Laboratory of Magnetic Materials, NFA, Institute of Physics, University of Brasilia, Brasilia, DF 70910-900, Brazil

J. J. A. Medrano
Institute of Physics, University of Brasilia, Brasilia, DF 70910-900, Brazil

M. C. Mathpal · J.-R. Maze
Instituto de Física, Pontificia Universidad Católica de Chile, Casilla 306, 7820436 Santiago, Chile

S. K. Sharma
Department of Physics, Central University of Punjab, Bathinda, Punjab 151401, India

S. K. Sharma et al. (eds.), *Harnessing Materials for X-ray Based Cancer Therapy and Imaging*, Nanomedicine and Nanotoxicology,
https://doi.org/10.1007/978-3-031-04071-9_1

1 Introduction

Since the development of nanoscience and its application in technology, so-called 'nanotechnology', from industry to biomedicine, nanomaterials and the relevant instrumental devices are the centered point of research. The advancement in each technology is a natural process in research which gives more precise, accurate and updated information's, and the methods to apply to the practical use. In particular, biomedical imaging is a focal technique at the in-vivo anatomic, structural, and functional visualization of inside-organs in a non or minimally invasive way. X-ray imaging is established as a strong imaging technique since the discovery of X-rays in 1895. Since then, a novel imaging techniques based on X-rays, such as radiography, fluoroscopy, computed tomography (CT), and single-photon computed tomography (SPCT) are developed which requires extremely sensitive materials/scintillators to enhance the image quality while minimizing radiation induced health risks to patients [1–5]. Recently, positron emission tomography (PET) showed its highly sensitive nature at the picomolar level that allows in-vivo molecular-imaging-based precise diagnosis.

Scintillators are energy conversion materials which absorb and translate X-rays radiations into the visible light region. Control Synthesis of novel X-rays induced scintillators tuning their luminescence properties is a rising field of current research. In this scenario, the idea of integrating the quick response toward X-rays with big absorption cross-section stemming from the thickness and relatively high mass density exhibited a good sensitivity in single-crystal perovskite-based scintillators under keV X-ray radiation. The lead-halide perovskite single crystal scintillators display a short absorption length and high detection efficiency to X-rays [6]. On the other hand, organic scintillators are observed having a weak detection of high-energy radiations because of their relatively low density of chemical constituents [7]. Organic crystals like naphthalene, stilbene and anthracene showed very weak detection capacity of higher-energy X-rays [8, 9]. However, they possess high attenuation constants that help them to act as excellent scintillator candidates for β rays and hot neutrons. To enhance their detection, heavy metal ions can be adopted to construct organic–inorganic based scintillators because of high energy resolution and energy-conversion efficiency of these metal ions [10]. Thus, this chapter presents a brief overview of techniques used in medical imaging, namely, radiography, fluoroscopy, angiography, and computed tomography as well as recent developed X-ray detectors/scintillators which show convincing results in terms of sensitivity and serve as an excellent candidate for medical imaging.

2 An Overview of X-ray: Discovery and Road Towards Biomedical Imaging

With the discovery of X-rays on 8 November 1895, the great revolution in the cognition of physical world is started. The discovery of X-rays was interesting as it was found incidentally while Wilhelm Conrad Rontgen was studying the behavior of cathode rays in Hittorf-Geissler-Crookes (HGC) tubes at his own laboratory. While busy with his experiments, unknowingly one day he observed that some crystals lying close to the HGC tube had become intensely fluorescent produced by a hitherto unknown radiation. After the spent myriad of breathless night, he confirmed that this could not be due to cathode rays; cathode rays are fully absorbed either by the glass wall of the tube, or by the air and thus introduced as an X-rays. The fluorescence stimulation in different crystals depends upon the voltage used, for instance, fluorite is a fine and suited crystal for 'soft' cathode rays, whereas barium platino cyanide fluorescing strongly under the bombardment of 'hard' cathode rays. The high energy X-rays, also referred as 'hard' X-rays, contain the component of short wavelength that amplify the penetration into thick objects or those with large object densities. Similarly, the low energy X-rays, referred as 'soft X-rays' component comprises the longer-wavelength X-rays which enhance the image contrast. The 'soft X-rays' are responsible to produce beam hardening corrections that can be applied to reduce their effects on the resulting X-ray image [11, 12]. The X-rays was the first in a series of three discoveries; X rays, uranium rays, and the electron, i.e., the study of the discharge of electricity in gases. These three physical discovery have immense contribution on the transformation of physical world of nanoscience and nanotechnology. The X-rays originate from the bright fluorescence on the tube where the cathode rays strike the glass and spread out. The point of origin of the X-rays moves in straight lines by a magnetic field, and their absorption depends on the material through which they pass, but the X-rays themselves are insensitive to the magnet. In principle, X-rays are produced by ionizing a target source, such as tungsten, with an electron beam at very high speed and retarded instantly. In this process, the electrons are discharged from a cathode and accelerated toward an anode by a high voltage potential between the cathode and anode. once the electrons strike with the anode, they start to decelerate accompanying by the emission of electromagnetic radiation. The energy spectrum emitted from the X-ray tube is a function of the voltage potential, target material, the angle at which the electron beam strikes with the target, the angle at which the X-rays are observed, and the material used for the X-ray tube window [13–15].

After the discovery of X-rays and its experimental verification, Roentgen's and Dr. Henry W. Cattell, Demonstrator of Morbid Anatomy at the University of Pennsylvania have demonstrated the X rays to locate bullets in human flesh and photograph broken bones and confirmed their importance for the diagnosis of kidney stones and cirrhotic livers, stating that "The surgical imagination can pleasurably lose itself in devising endless applications of this wonderful process." This was the key step to move forward the application of X-rays in medical sciences. Röntgen

demonstrated the medical use of X-rays with taking a picture of his wife's hand on a photographic plate formed. It was the first photograph of a human body part using X-rays. The first use of X-rays for a surgical operation was implemented on February 14, 1896 [16]. This success of the first medical applications contributes not only to the lives of humanity but also open the industrial possibility in medical science and technology. Imaging techniques is one of the great and finest achievement of physical science which provides an interface between vision and intuition. Especially, biological imaging has taken a wide space in human lives, not only to understand the fundamental biology in nature but also due to extensive use in medical science, i.e., biomedical imaging in view of its ability to aid analysis and diagnosis through X-ray images at the molecular and cellular levels [5, 17]. X-ray imaging is a noninvasive measurement techniques used extensively for the evaluation of static objects, visualize and characterize the complex internal structures. The several techniques can be used to detect an X-rays. Initially, it was detected through film-based techniques; however, with the time, researcher successfully designed a new system where digital detection can be achieved through electronic detector [18]. There are two types of detectors: direct conversion and indirect conversion detectors. In case of direct conversion detectors, X-ray photons are directly converted into an electrical charge with the help of an X-ray photoconductor (e.g., amorphous selenium). On the other hand, in case of indirect conversion detectors, first a scintillator converts incident X-rays to visible light, and then this obtained light is converted to an electrical signal through a photodetector. In both cases, the output signal from these devices is sensed by an electronic readout mechanism with an analog-to-digital converter to yield digital image. The X-ray imaging systems, for example, old computed tomography systems, scintillators are used to convert X-rays to visible light; the visibility of light depends on the X-ray energy. The linear scintillator simply facilitates for the electronic absorption of individual signal to quantify the X-ray intensity of a fan beam through a horizontal plane [19, 20].

3 X-ray Imaging and Application in Medicine

The use of X-ray in medical imaging is under two categories: structural imaging, which reveals anatomical structure i.e. imaging of bone, teeth, microcalcinations, lungs, and orthopedic devices, and functional imaging which track the main changes in biological function, such as metabolism, blood flow, regional chemical composition and biochemical processes. However, endogenous soft tissue types are difficult to distinguish using conventional X-ray projection imaging. Distinguishing tissue types for functional imaging requires either exogenous contrast agents (e.g., radiopaque agents to view vasculature and flow in angiography), or technique that are more sensitive to tissue differences (or both).

3.1 Radiography

Radiography is an application of X-ray imaging used in medical science. The foremost aim of radiography is the inspection of ruptures, cracks the internal structures of the body and their effects/changes in the skeletal system. In addition, this technique is used to perceive the changes of a bone's consistency or density, e.g., in case of osteoporosis or bone cancer. Radiography creates two dimensional projection images by exposing an anatomy of interest to X-rays and record the photograph of the X-ray attenuation map of an object when passes through the object. X-ray images are processed in a similar way of conventional photographic film in which shadow of an object are analogized. The lighter shadow images are related to the object areas of greatest density. The X-ray attenuation map of an object/materials has great role on the development of contrast in the radiograph and hence better images quality. The obtained contrast in the radiograph usually reduced by the consequence of the X-ray absorption and X-ray scattering. The X-ray absorption is always varying with the X-ray energy level, whereas X-ray scatter cause a general fogging of the image; as a consequence, reduces the brightness and sharpness, clear contrast, and the resolution. Such scattering is possible to reduce by passing the X-ray through a metal filter before to reach the object of interest that, obviously, lessen the quantity of soft X-rays reaching to the object [15]. On the other hand, advance digital detectors use to capture the X-ray intensity that produce images. Digital radiography improved the sensing capacity of 2D sensor arrays and computer power of receiving, processing, and displaying the large data sets. The advantages of digital radiography, as compared to the conventional film, is the speed of image obtained and the pliability in manipulating and accumulating those images.

There are several techniques of radiography imaging process which are used for a specific purpose from industrial technology to nanomedicine; among them, X-ray radiography for flow visualization (XRFV) and Flash X-ray radiography (FXR) are widely used. The XRFV is extensively used in myriad industrial applications, such as power generation, pharmaceutical production, fuel production, and mineral and powder processing. The working mechanism is based on gas/liquid flowing through a granular bed at an ample velocity to suspend the particles, where these granular beds have ability of uniform mixing, low pressure drop, high heat and mass transfer rates. On the other hand, the flash X-ray radiography (FXR) is an imaging process where strong burst of irradiation is induced for a second that records a high-speed events obscured by light. In addition, FXR helps to seize the images of voids inside opaque objects that are scrap of these dynamic events. These FXR are often used in medical imaging for biological studies [21–23].

3.2 *Fluoroscopy*

The fluoroscopy technique is a very essential in minimally invasive intercessions, where the different tool such as catheters and endoscopes need to be guided to operate the system without direct visual contact to the intercession region. Moreover, this is the technology to visualize internal organs/vessels, for instance arteries or veins using scintillators as a contrast agent; as a result, fluoroscopy is also referred as a positive contrast technique having a low background and highly sensitive to low elemental concentrations [24, 25]. In principle, during the absorption of X-ray photon by an atom, small part of its energy reemit as a secondary X-ray fluorescence (XRF). In this process, binding energy and nuclear charge are key factors; the binding energy is proportional to the square of nuclear charge and the emitted photon energy is characteristic of each element. The scanning of the specimen and acquisition of X-ray yields quantitative topographical maps for a wide range of elements, that allow the quantitative elemental analysis, including most biologically relevant transition metals. Taking an advantage of the elemental quantification/composition using nuclear charge of elements [26], this technique is applying to find the metal toxicity [26, 27], uptake and distribution of metallopharmacueticals [28], intracellular elemental distributions in biological samples[2, 29–31], and in vivo to non-invasively evaluate the concentration in the bones, human skin, and iodine in the thyroid [32–34]. The image from a fluoroscopy sequence can be depicted by the placement of the two electrodes and wires of a heart pacemaker. A precise and accurate clinical setup is very essential for a minimally invasive surgery where the X-ray imaging unit is given by a C-arm scanner that can be freely positioned around the patient. Conventional radiography typically refers to the acquisition of a single or small number of X-ray projection images for a specified view. In contrast, fluoroscopy describes a sequence of radiographic images acquired periodically at a certain frame rate. The X-ray source can either be triggered for each frame or simply provide a constant radiation exposure to the region of interest. Potential X-ray detectors can be image intensifiers. The frame rate is typically limited by the acquisition speed of the detection system. For image intensifiers, it is given by the inertia of the final fluorescent screen. In practice, frame rates of 30 frames per second are possible. However, rates are often reduced for dose reasons. In brief, fluoroscopy is a promising procedure because it is less invasive, substantially reducing the risk of infection or skin injury due to iatrogenic radiation, compared to conventional surgical procedures, being able to use dose metrics to develop adequate follow-up and management plans for the patient [35].

The use of the fluoroscopic technique came after the discovery of X-rays, where in the beginning the operating mechanisms of these equipment was limited due to technological factors: such as low-quality film emulsions and X-ray tubes that were not very reliable in their functioning. For this reason, fluoroscopy appeared as a more promising and probably more important alternative than radiographic techniques. Subsequently, the equipment improved and fluoroscopy began to occupy an extremely important role in imaging examinations and that it is still in force today, in other words, the study and detection of moving parts, dynamic examinations, interventionism, angiography, make this technique be of great acceptance

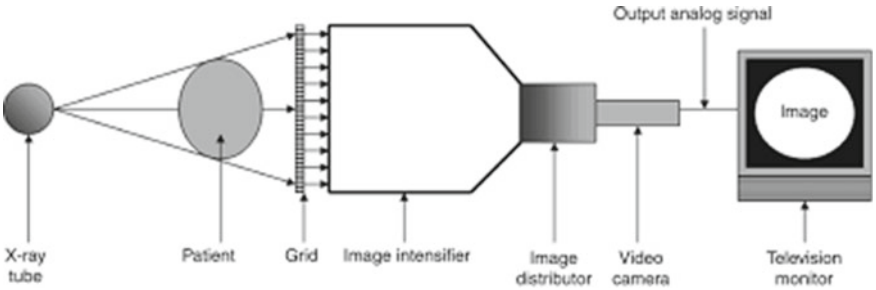

Fig. 1 Representation of a fluoroscopy equipment with image intensifier. Reprinted with permission of Ref. [38]

[24, 25, 36]. The main difference between radiography and fluoroscopy is that the latter uses a much lower X-ray fluency rate, but for a much longer time. Through this technique a continuous image is produced allowing the observer to see dynamic changes within the patient such as moving organs or flow of contrast media through blood vessels, digestive system. The principle of fluoroscopic imaging is in the ability of X-rays to cause fluorescence in a phosphor-like material. A fluoroscope basically consists of two components: An X-ray tube and a fluoroscopic screen. The tube and the screen are mounted facing each other in an aligned way, (see Fig. 1). In this way the operator moves the fluoroscopic screen along the patient and the tube follows the screen. X-ray photons that pass through the patient interact with the screen, producing photons of light that reach the observer [37].

Certain limitations must be considered due to this arrangement, such as, for example: images with a very low brightness, three or four orders of magnitude lower than that of a conventional radiograph. The possibility of increasing the X-ray rate is not feasible either because this would mean doses that are clearly intolerable for patients and also very high for the observer himself. Therefore, the fluoroscopic image can only be viewed without ambient lighting, in the dark, with the consequent loss due to the vision characteristics of the human eye and the inconvenience of adaptation to darkness. The result is a very poor quality image. The only way to significantly improve this quality without excessively increasing the doses to patients is by using a system that amplifies the light from the screen: the image intensifier.

Fluoroscopy is demonstrated in several types of experiment including cardiac catheterization [39], lumbar puncture, arthrography, placement of intravenous catheters, and biopsies. Further applications of fluoroscopy include foreign body localization, injecting image-driven anesthesia into the spine, and in percutaneous vertebroplasty [40]. The use of nanoparticles have shown very promising results that suffused into bio-degradable filters made up of poly-p-dioxanone (PPDO) could amend device radiopacity without any unexpected effects on device efficacy and safety, in swine models [41]. This demonstrates the continuous effort to improve procedures and add the use of new nanomaterials to optimize results. The most common applications are:

In Diagnosis:

- Digestive system: swallowing studies, esophagograms, intestinal transit, laparoscopies, barium enema, transcutaneous liver biopsies, enteroclysis.
- Urology: cystography, diagnostic percutaneous nephrostomy, percutaneous excretory urogram.
- Gynecology: hysterosalpingography.
- Neurology: myelograms.
- Cardiology: angiograms of vessels of the lower extremities, heart and brain; intracardiac electrophysiological study (EPS).
- Traumatology: arthrography, post-surgical control.

In Treatment:

- Placement of endoprostheses: esophageal, biliary, urethral stents, intravascular stents.
- Infiltrations: especially common in intra and periarticular drug infiltration (anesthetics, corticosteroids, contrast solutions).
- Dilation of vascular, digestive or urological stenosis.
- Guided surgery: biopsies, vertebroplasties, tumor removal (especially in delicate locations), kidney surgery, nephrostomy, placement of pacemakers and cardiac defibrillators, angioplasties, urological surgery (especially in retrograde pyelography).

The use of fluoroscopy is usually considerable in regards of safety concerns. However, the risks arise due to the accumulated radiation from number of X-ray test or treatments for a long period [42]. For a fluoroscopy patient, it is important to consider whether the patient suffers from any type of allergies to the substance to be administered or any history of allergic reactions. Patients who are allergic to any remedy, iodine, latex, or contrast environments are at a higher risk of developing an allergic reaction. It is not recommended that pregnant women be exposed to this type of procedure with fluoroscopy due to the risk that it can affect the fetus.

3.3 Angiography

Angiography is a technique that consists of filling the vessels of the circulatory system with a contrast agent, that is, a good absorber of radiation that produces a visible shadow in the image. This substance is injected into the area to be explored, using needles or guiding a catheter under fluoroscopic control. To perform the test, anesthesia is applied to the site where the catheter will be inserted, which is a small tube that is directed by the doctor to the site where you want to see the blood vessels, which is usually inserted in the groin or neck. After the catheter is inserted into the site to be tested, a contrast agent is injected and then several X-rays are taken on the X-ray machine. The contrast liquid, when exposed to X-rays, will be shown on the monitor image with a different color from the images taken, which allows observing the

patient's circulatory system. During the exam, the patient remains awake, but since it is necessary to remain as still as possible, the doctor may apply medication to sedate the patient. This procedure can take about an hour. After this time, the patient does not necessarily need hospitalization, since general anesthesia is not used. In some cases, it may also be necessary to suture and place a dressing where the catheter was inserted. At present we can find more modern equipment, where characteristics such as road mapping (in which the interventional doctor can use images with contrast and digital subtraction previously acquired to use them as a way to introduce catheters with diameters less than 1 mm without using more contrast), have greatly facilitated angiographic and interventional procedures [43, 44].

Another advantage currently used is the use of pulsed fluoroscopy, where the duration of the examination is much shorter and also the amount of dose administered to the patient is less, thus obtaining a good quality image.

In general, this equipment consists of a C-arm suspended from the ceiling or anchored to the ground that incorporates the X-ray tube and the image receptor system. This arch can be moved in almost all directions to allow as many views of the patient as possible. This is placed on a lifting table, with a flat, floating and sliding tabletop that allows easy access to the patient. A mobile device with two or more TV monitors allows the specialist to follow the image in real time while performing the examination or to view the dynamic series previously obtained (see Fig. 2).

Currently there are high-end models where the use of dynamic flat panels as image receptors has notably improved the performance of this equipment, considerably improving the quality and contrast of the image, in addition to the fact that the mass and volume lightening of the arc allows a remarkable agility with faster and more precise movements. Relatively recent developments such as so-called rotational angiography in which the image receptor-tube assembly (or assemblies) rotates around the patient at high speed, taking pulsed images while a contrast medium is injected into the patient, have been incorporated into current teams. In this way the images are processed and displayed as a video sequence with the advantage that the vascular tree can be seen from different orientations with a single injection of contrast [46, 47]. One step further is the possibility of performing a 3D reconstruction of the vascular tree. In recent years, the equipment has incorporated the possibility of obtaining tomographic sections, as well as those obtained with a computerized tomography, using the digital image detector itself.

In a large number of surgeries, fluoroscopy or X-ray imaging is required during the surgeries. The transfer of the patient to obtain an X-ray, or the installation of a permanent X-ray equipment, being unfeasible, which can make interventions in which X-rays are not required due to space issues. For this situation where the use of fluoroscopy is necessary to guide a catheter or an endoscope, there are mobile radio surgical arches. They are so named because of the appearance of the X-ray tube and image receptor as a C-arc (See Fig. 3), with both parts always aligned and at a fixed distance (90–100 cm). In this way, the patient can be positioned between the tube and the intensifier and access to the examination site is relatively free. This arch is mounted at the end of an extendable arm anchored to the foot of the equipment that includes the X-ray generator and the console with the controls. Said foot has wheels

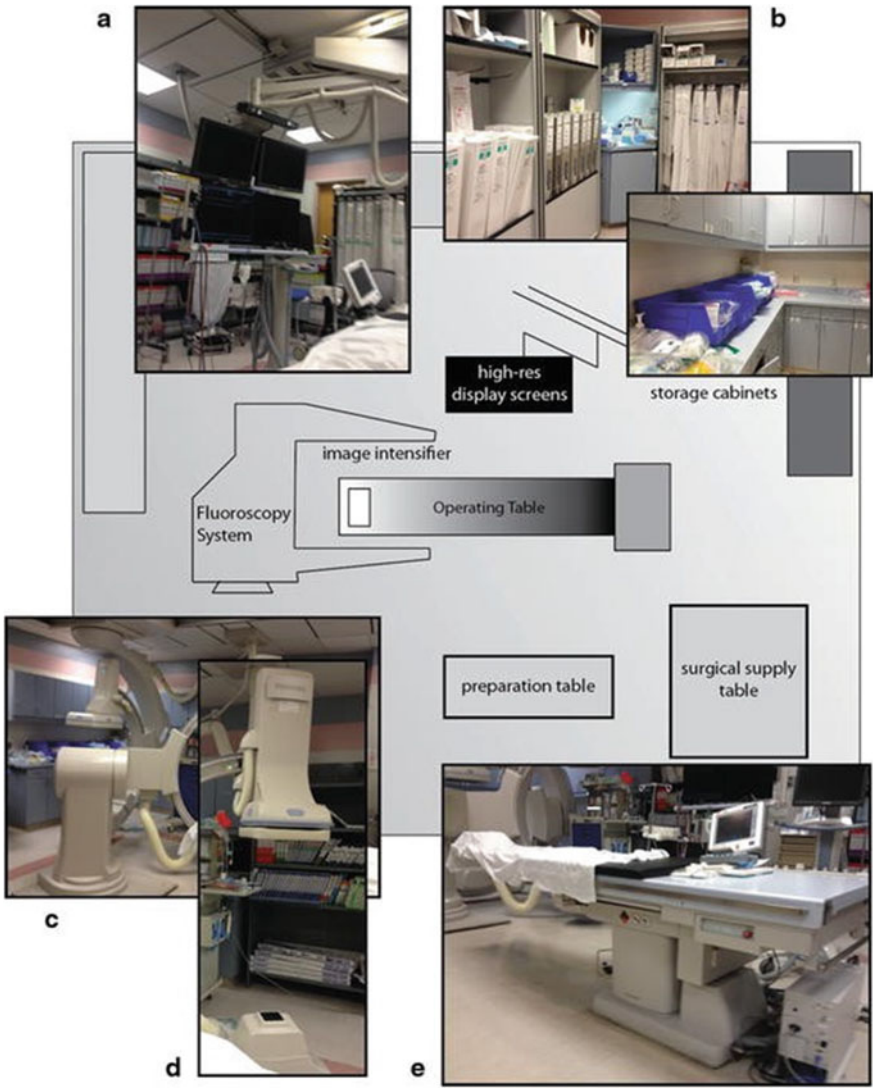

Fig. 2 Representation of an angiography equipment. Reprinted with permission of Ref. [45]

which allow the movement of the whole equipment. Due to the need for space and their good performance, all current arches incorporate high-frequency generators, which also allows the use of pulsed fluoroscopy.

The use of nanomaterials is increasingly present in biomedical applications. Composite of nanoscale zero-valent iron in ordered mesoporous carbon (nZVI@C) are being used in trials to improve image quality in Magnetic Resonance Angiography studies. In addition, this material did not show deleterious effects on cells [49].

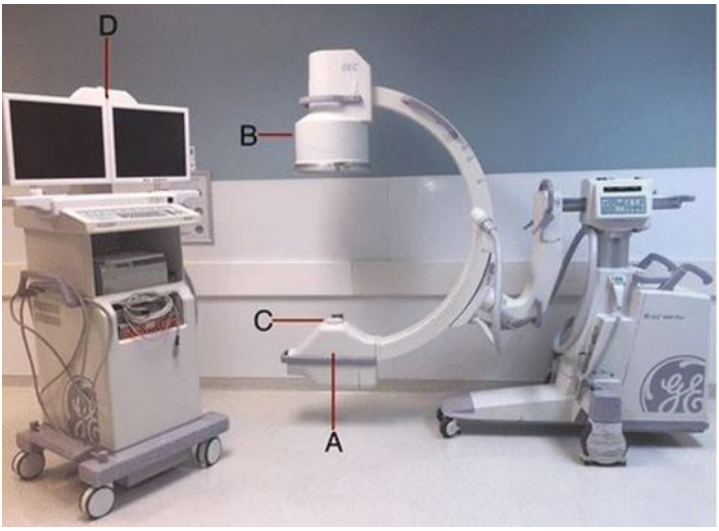

Fig. 3 Mobile C-Arm used in angiography; **A** X-ray Tube; **B** Image Intensifier; **C** Collimator; **D** Display Monitor. Reprinted with open access permission Ref. [48]

Currently some kind of ferrites like as $ZnFe_2O_4$ are explored as the contrast agent for magnetic resonance angiography, due to his higher transverse relaxation time. First assays are being in rats. Results show an increase in image contrast using nanoparticles $ZnFe_2O_4$ smaller than 6 nm [50]. Procedures that use angiography range from intravenous or arterial injections to angioplastic techniques that use balloons, stents, and other devices to unclog blood vessels and reinforce the internal structure of damaged arteries. Modern angiography units are equipped with a variety of the latest developments in fluoroscopic imaging technology including C-arms with fully movable image receiver and tube and a complete digital image acquisition system. In the hemodynamic units in which the coronary tree of the heart is explored, it is usual to use very high fluoroscopy and acquisition rates (25 images per second and even higher) to avoid the loss of spatial resolution due to the movement of the heart. On the contrary, in vascular radiology equipment the acquisition rate is not so critical, but the size of the image receptor (intensifier or flat panel in the most modern equipment), since many of the examinations are performed in the abdominal area or in the trunk of the patient. The most common risk from this test is an allergic reaction to the contrast medium that is inserted; however, the doctor usually has medications ready to inject if this happens. In addition, bleeding at the catheter insertion site or kidney problems may also occur due to the contrast medium (nephropathy) [51].

3.4 Computed Tomography

X-ray computed tomography (CT) can provide unmatched information on the internal structure of materials non-destructively from meter scales to tens of nanometers in length. It takes advantage of the penetrating power of X-rays to obtain a series of two-dimensional (2D) radiographs of the object seen from many different directions. This process is sometimes called a CT scan [52]. CT should not be confused with conventional X-ray radiology, which also allows two-dimensional visualization, but with much less detail, because the different structures of the body are superimposed on the same image, because the radiation is emitted from a single image. diffuse shape. On the other hand, for CT a very well-directed beam is used and with a certain thickness, which depends on the size of the structure to be studied, and can vary from 0.5 mm to 20 mm. The development of new, more sophisticated equipment obeyed a need, since with the first scanners for clinical use, data was acquired, for example, from the brain in approximately 4 min, two contiguous sections, and the calculation time was about 7 min per image. Shortly afterwards, scanners applicable to any part of the body were developed; First they were axial scanners, with a single row of detectors, and from these it was moved to helical or spiral scanners, which later allowed the use of equipment with multiple rows of detectors, whose clinical use has reached wide diffusion today [52, 53].

Today, specially designed CT scanners are available for certain clinical applications. Thus, there are specific CT equipment for planning radiotherapy treatments. Another current example is the integration of CT scanners in applications that include various imaging techniques; for example, by hybridizing a CT scanner with a positron emission tomography (PET), or with a single photon emission tomography (SPECT) [54].

Axial computed tomography is the first equipment used or called “first generation”, they use parallel beam geometry and a translation-rotation movement. The X-ray beam is highly collimated and, after passing through the section of interest of the patient, it strikes a pair of scintillation detectors each coupled to a photomultiplier tube. The emitter-detector assembly, integrally joined, moves through 160 positions, thus obtaining different measurements [55]. The most recent equipment is often described as “rotation only” or “rotation-stationary”, since it is now only the X-ray tube that rotates around the patient while the detectors, which cover the entire 360° space, remain immobile during cutting (see Fig. 4).

Helical computed tomography has greatly improved CT performance. Some of the advantages of helical CT: scan time is shortened, and more consistent information is obtained to reproduce 3D images of the scanned volume. The main disadvantage of helical CT was the appearance of some associated artifacts (windmills, etc.) [57, 58]. Helical acquisition made it possible to obtain data from a large volume of the apnea patient, which was a prerequisite for the development of high-quality CT angiography. The displacement of the stretcher is generally expressed in relation to the nominal width of the beam (equal to the width of cut in single cutters); the quotient between the displacement of the stretcher in a 360° rotation of the tube

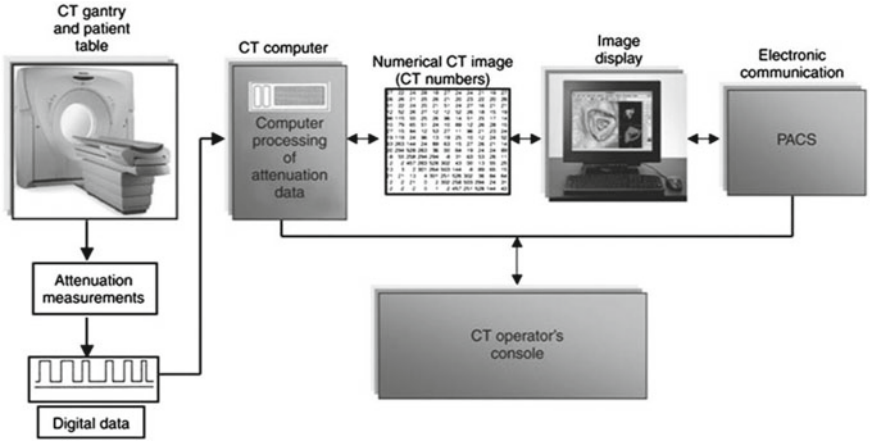

Fig. 4 Representation of computed tomography. Reprinted with permission of Ref. [56]

and the nominal width of the beam is called the pitch factor. Obviously, continuous scanning considerably reduces the exploration time, while allowing a more efficient use of the X-ray generating system. In return, as can be seen, the data collected in a complete revolution does not correspond exactly to any complete axial section, but the section moves continuously with the movement, also continuous, of the stretcher.

Multi-slice computed tomography, ten years after the introduction of helical CT, with the introduction of rapidly rotating multi-detector scanners, there was an enormous advance in CT technology that facilitated the emergence of new clinical applications. The first teams with 4 contiguous rows of active detectors, gave way to those with 16 and 64 rows respectively, which made possible the simultaneous acquisition of profiles of a large number of sections. In addition, the rotation time was reduced from 1–2 s, typical in single cutting equipment, to much lower values (0.3–0.4 s). Consequently, under these conditions it is possible to scan practically the entire body of an adult on inspiration with slice thicknesses well below 1 mm. With multi-detector CT equipment, acquisitions are usually made in helical mode. Exceptions are for high-resolution CT of, for example, lungs, and sequential acquisition on cardiac CT, either for coronary calcium calculation or for coronary CT angiography [59, 60].

An obvious difference between the different types of tomography can be observed in Fig. 5. It is possible to see the difference in tones in the images obtained, which allows more detailed information on the area of interest, allowing the doctor a decision on the most convenient treatment.

CT is used in diagnosis and in patient follow-up studies, in planning radiotherapy treatments. Diagnose different diseases and minor changes in various sectors of the human body. For example, a CT scan can evaluate a head injury or, because of its quick results, help find strokes. In addition, the procedure helps to detect tumors and infectious processes of different organs. The exam also detects important

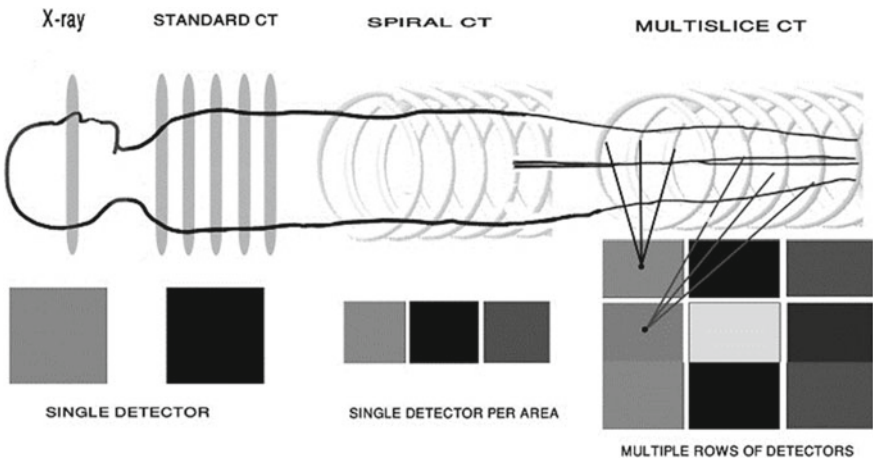

Fig. 5 Difference between techniques using computed tomography and X-ray. Reprinted with open access permission Ref. [61]

warning signs, such as bleeding, aneurysms, perforation of intestinal loops, and even heart attacks. It is well known that there is a growing concern for the care of the environment, this reflects efforts in nanobiotechnology, that is developing new processes for the synthesis of nanoparticles (green synthesis). Was reported the use of aqueous leaf extract of barley leaves during process of synthetic to obtained new gold nanoparticles (BL-Au), taking advantage of the fact that the extract of barley leaves has properties that act as a reducing agent during the synthesis process. Results of this assay using BL-Au nanoparticles in computed tomography with zebra fish showed Brightness image was still much stronger than Ultravist (component usually used in this process) [62]. Another interesting work used Au nanoparticles as contrast agent for computed tomography in mice, with different sizes of nanoparticles and found that larger Au nanoparticles provided strong liver and spleen contrast [63].

All X-rays deliver ionizing radiation, which has the potential to cause natural impacts within the human body. For patients, these biological impacts can run from an expanded hazard of cancer at some point in life, to conceivable unfavorably susceptible responses or kidney disappointment from contrast media. Beneath a few uncommon circumstances of delayed presentation to expansive dosages, x-rays can cause unfavorable wellbeing impacts such as blushing of the skin (erythema), harm to skin tissue, hair misfortune, cataracts, or birth abandons (in the event that they consider is carried out). carried out amid a pregnancy). For this reason, it is critical that CT checks are constrained to as it were those cases where the advantage that can be gotten essentially outweighs the increased hazard. This is often particularly genuine for children, who are more sensitive to ionizing radiation and have longer life anticipation and so have a generally higher chance of creating cancer than adults [64].

4 High Energy X-ray Sensitive Materials for Medical Applications

The strong penetrating power of invisible high energy X-rays allows them to scan the object and display the internal parts/structure/composition in medical imaging [65, 66]. In X-ray based imaging, Image contrast results from the variable signal detected when rays are absorbed, preventing the receptivity of the various organs/subjects to the radiation. Albeit, such rays are hardly perceived by ordinary photographic substrates, so studies are devoted to the search of scintillating materials with the properties of efficiently absorbing these rays and converting the absorbed X-rays into photon radiation emitted in the visible light range. Scintillators are special energy conversion materials that can absorb X-rays/γ-rays and convert them into the visible light range [67]. Although scintillators are unable to produce medical X-ray images straightly, they are advantageous due to their ability to reduce the radiation dose required for imaging. It is clear from the definition of 'high energy' that higher atomic numbers (Z) metals ion are needed to achieve high stopping power and noteworthy scintillation performance since they have high energy resolution and energy-conversion efficiency [10, 68].

4.1 Perovskite-Based Sensitive Materials

Perovskite-based nanomaterials (PNMs), such as $CaTiO_3$ and its diverse composition (ABX_3 where A and B represent as cations and X as anion) have been investigated persuasively in the last decades due to their tunable photoelectric properties, luminescent and electrical performance which allow these materials to be used in wide range of medical imaging [69–71]. Different energy conversion phenomena can be discussed in such X-ray perovskite-based detectors; in scintillator based detector, energy conversion takes place from X-ray to UV–Vis photon via down-conversion [72]. In addition, the absorption material has limited carrier diffusion length by which these materials are recommended to avoid in X-ray based scintillators [73, 74]. Considering those materials which exhibit limited/short absorption length but high detection efficiency to X-rays, Lead-halide based perovskite single-crystals are promising scintillators. The quick reaction toward X-rays with large absorption cross-section originated via physical factors, such as, thickness and relatively high mass density, made perovskite scintillators promising materials to enhancing the detection efficiency under keV X-ray radiation [6]. However, these materials show their better performance only on low temperature since they are sensitive to open environment, i.e., air and humidity since they are sensitive to these factor (air and humidity) [10, 75]. As compared to bulk perovskites, perovskites nano-scale materials have been demonstrated as a better processing capability for the fabrication of multifunctional thin films, flexible devices [76]. Furthermore, they exhibit a superior optical and electromagnetic properties because of their quantum effect and small-size effect

[77]. The use of high energy scintillators varies on the required fields. Particularly in X-ray imaging, following points should have to be considered: (a) high absorption coefficient which provides a considerable quality of imaging with reducing the dose amount, (b) highly luminescence yield which reduces the noise signal, (c) decay time should adjust in the range of CT scanners in $\geq$10 kHz, (d) absence of afterglow that causes sickle artifacts in the imaging, and (e) Low temperature dependence of the LY.

Several pattern of Pb-halide perovskites such as bulk crystals, thin films, nanoparticles and quantum dots can be prepared by chemical routes instead of ultra-high vacuum technique; which minimizes the cost within a reasonable range. As it is established, however, that Pb element is toxic that led towards the health threats in biomedical use. Besides, low resistance to the humidity and temperature reduces their sensitivity that evidently limit the application of interest. Recently, organic–inorganic hybrid Pb-halide perovskite-has been prepared that exhibits an excellent scintillator in view of their low preparation cost, high light yield, short decay time in the nanosecond range, and low inherent trap density [6]. Methylammonium Pb based perovskites (MAPbX3) have demonstrated a significant scintillating performance for luminous devices and high-sensitive detectors in the visible range [78–80]. Saidaminov et al. [81] have reported the novel hybrid organo-lead tri-halide perovskites, MAPbBr3 and MAPbI3 in hot solutions, prepared by controlling the solvent, temperature and other parameters. They found that these material show carrier transport properties similar to those grown by the usual cooling or anti-solvent vapor-assisted crystallization techniques. The authors stated the 'quantum leap' in crystal growth rates of these scintillators presents a major breakthrough in the research area of perovskite single crystals enabling the wide applications from medical imaging to industrial technology. Moreover, Wei et al. [82] have synthesized sensitive $MAPbBr_3$ single-crystal X-ray detectors with a record $\mu\tau$ product of 1.2×10^{-2} cm^2 V^{-1} and the lowest surface recombination velocity of 64 cm s^{-1}. Impressively, this material exhibited an excellent optoelectronic property as compared with those for CdZnTe. It was synthesized by the solution growth method which take an advantages of low cost, large scale and faster growth rates than the conventional routes, i.e., vapor deposition method adopted for CdZnTe crystal growth. The performed experiment of a charge collection efficiency up to ~33–42% for UV–vis light, and ~16.4% for hard X-ray photons which facilitates the ability to direct conversion of high-energy X-ray into collectable charges with a high sensitivity of 80 μC G y_{air}^{-1} cm^{-2} and a lowest detectable dose rate of 0.5 $\mu Gy_{air} s^{-1}$, which meets the practical needs of medical diagnostics. They believed that these findings offer an effective way to engineer the trap density of the hybrid perovskite material to increase the device charge collection efficiency for photodetectors. Later following this work, Wei W. and co-workers [83] designed the Si-integrated $MAPbBr_3$ through low-temperature solution-processed molecular bonding method in cooperation with brominated APTES (3-aminopropyl triethoxysilane) molecules. The insertion idea of this layer was to reduce the dark current which is crucial for a detector to sense very low X-ray. It is found, as anticipated, that a momentous lessening in dark current at higher bias, detecting a really low X-ray (8 keV) measurements rate of <0.1 μGy_{air} s^{-1} with a high affectability of 2.1×10^4 μC G y_{air}^{-1} cm^{-2}. Further, they appeared that the X-ray dosage to patients utilizing the

created direct finder cluster can be drastically decreased by 15–120-fold. The result gotten here is a few orders of magnitude superior than the state-of-the-art commercial α-Se X-ray locators, clearing the way for the commercialization of perovskite X-ray finders for therapeutic applications. This strategy gives an effortless way to coordinate MAPbBr3 single gems onto different by and largely utilized substrates at moo temperatures in arrangement, which opens an unused road for the application of perovskite materials in much broader areas, such as active-matrix flat-panel imagers and flat-panel shows.

The lanthanides with proper energy state, i.e., the rare earth (RE) doped scintillators have exhibited satisfactory properties [84]. Recently, scintillators of CaI_2: Eu^{2+} with doping RE [85] and LuI_3: Ce^{3+} [86] have achieved ray output of more than 100,000 photons per MeV. Similarly, Sr^{2+}, Ca^{2+} co-doped $LaBr_3$: Ce^{3+} scintillator show an ultrahigh energy-resolution [87], while some scintillators, for example, Ce^{3+} doped $PrBr_3$ [88] and Nd^{3+} doped LaF_3 have very short scintillating decay time of 6 ns. Interestingly, these scintillators emit photons in the range of ultraviolet, visible, or near-infrared when excited by X-rays/γ-rays, so that are considered as potential scintillating materials for medical imaging [89]. Likewise, to use lanthanide-based scintillators for CT imaging, Tb^{3+} doped LaF_3-Rose Bengal (RB) scintillators are functionalized with a silica layer for the pathologic diagnosis of cancer [90]. It is observed that the shell-thickness of the silica layer was controllable which given a uniform measure, great biocompatibility, colloidal soundness, and photostability. It is found that once the nano-scintillator infused into the tumor location, the flag escalated expanded significantly. The measured X-ray constriction control outperforms the commercial CT differentiate instrument (Ultravist® 300), which makes it a perfect CT differentiate specialist for deep-tumor determination. In spite of the fact that promising in CT imaging, more tests are still required to encourage confirm the photodynamic restorative efficacy of the Tb^{3+} doped LaF3-RB scintillating fabric by X-ray actuation. Investigating multiplexed scintillators has gotten to be an inquire about hotspot for the development of double show imaging devices.

5 Highly Sensitive X-ray Detector: Organic and Inorganic Materials

Xu et al. [3] have developed a new zero dimensional (0D) organic manganese (II) halide hybrid $(C_{38}H_{34}P_2)MnBr_4$ which exhibit highly efficient green emission upon photo and X-ray excitations. It is observed that the X-ray image of $(C_{38}H_{34}P_2)MnBr_4$ single crystal is more brighter than Ce:LuAG indicating that $C_{38}H_{34}P_2MnBr_4$ is more sensitive to X-ray irradiation than Ce: LuAG. Further, the scintillator response to X-ray dose rate, the radio-luminescence (RL) intensities have been investigated under various X-ray dose rates for $(C_{38}H_{34}P_2)MnBr4$ and Ce:LuAG. This single crystal scintillator shows discernible scintillation properties with amazing reaction linearity to dosage rate, tall light abdicates, and low detection limits. Interestingly,

the X-ray scintillation properties were found to be prevalent to those of metal halide perovskite nanocrystals and most of today's commercially accessible scintillators. X-ray imaging was moreover effectively illustrated with tall determination. The low-cost, simple planning, ecologically neighborly, and state-of-the craftsmanship glitter execution make this natural manganese (II) half breed $(C_{38}H_{34}P_2)MnBr_4$ an exceedingly promising scintillator for commercial applications. The authors believed that this work could be a new way to explore new low-cost, high-performance eco-friendly hybrid materials for radiation scintillators. Although, scintillators have a tunable properties in visible region owing to their abundant electronic states, adjustable bandgap, high detection efficiency and relatively lower reabsorption to X-rays [91–93], pristine perovskites exhibit some intrinsic deficiency. For instance, some halide PNMs have demonstrated a limited adaptability of optical and electrical performances in addition to poor stability for light, heat, oxygen, humidity and aggregation and phase transition [94]. Researchers are still trying to add external doping ions into PNMs to overcome these drawbacks [70].

The design of novel scintillators which allow the medical detections under lower X-ray radiation dose with faster evaluation is still challenging and large area of investigation still need to be addressed. Organic nanocrystals such as stilbene, naphthalene and anthracene showing high attenuation-constant which can be used as scintillating materials for β-ray; however, they show a poor efficiency on X-ray detections [8, 9]. Based on organic framework, metal organic frameworks (MOFs) scintillators exhibit noteworthy energy conversion efficiency to X-rays which opens tunable platform for several application [95]. The organic emitters allow them to respond quickly to X-rays as compared to conventional available inorganic scintillators [96]. The strong green light emission actuated by the charge-transfer from ligand to metal, advocates that the UVI materials are anticipated as a proficient scintillating candidate for X-ray detection and the perceptible light emission in a uranyl-organic system (SCU-9) are exceptionally promising highlights for down to earth applications in therapeutic imaging areas. SCU-9 assist appears the prevalence of decreasing the non-radiative unwinding within the prepare of excitation, which advance makes strides the transformation productivity. The emission escalated appears a basically direct relationship with the uncovered X-ray measurements, and this parameter is comparable to that of the commercial scintillator CsI:Tl. In expansion, SCU-9 moreover shows diminished hydroscopicity, improved X-ray radiation resistance, and decreased effectiveness [97].

Thirimanne et al. [98] have synthesized a hybrid 'inorganic in organic' X-ray detector which demonstrated promising sensitivities of 1712 and 58 $\mu C\ mGy^{-1}\ cm^{-3}$ for soft and hard X-rays respectively. In addition to this, due to the flexibility of the detectors, they show a high sensitivity of 300 $\mu C\ mGy^{-1}\ cm^{-3}$, recommending its potential for dosimetry and bio-imaging in non-planar architectures. The made strides X-ray affectability could be a result of affect ionization, and an upgraded way length due to Mie diffusing and the proficient division, and transport of these by the BHJ-NP engineering coming about in high-charge collection efficiencies (>60%). Based on this concept, a preparatory level board imager has moreover been illustrated. The strategy of coordinate discovery and imaging, combined with low fetched,

adaptability and versatility for large-area fabricate, makes strides on current strong state X-ray finder execution by 2–3 orders of magnitudes, beneath low voltages, whereas conveying novel properties reasonable for an extend of current and already unexplored discovery and imaging applications.

Lee and co-workers [99] have studied organic–inorganic X-ray detectors by adding inorganic quantum dots (QDs) to the organic active layer which results the improved sensitivity due to combined interface properties, i.e., excellent physico-chemical stability, excellent carrier mobility, and efficient photon absorption on the organic polymer interface. The inner organic active layer consisted of a conjugated polymer P3HT and fullerene derivatives PC70BM to which indium phosphide (InP) QDs were added by changing the size and amount of InP) QDs. The sensitivity of the detector was extracted during X-ray exposure according to the QD size change (4–12 nm in diameter). It was observed that the sensitivity decreased with the increased QDs size. Moreover, the absorbance of the active layer decreased when the size of QDs exceeded 4 nm which reduces the solubility and dispersion of the QDs in the organic active layer. Therefore, the detector with the P3HT:PC70BM:InP QDs (4 nm diameter) showed the highest sensitivity, of 2.01 mA/Gy·cm2, showing that the sensitivity was improved by 44.60% over that of the P3HT:PC70BM detector. On the other hand, there is another way to further improve the sensitivity by varying the amount of QDs keeping the QDs size fixed to 4 nm in diameter. It was observed that the most noteworthy affectability of 2.26 mA/Gy·cm^2 gotten from the finder P3HT:PC70BM:InP QDs (1 mg) dynamic layer. In expansion, the most noteworthy versatility, of 1.69×10^{-5} cm^2/V·s, was gotten from the same locator. The changed sum of InP QDs within the P3HT:PC70BM natural dynamic layer changed the surface morphology, subsequently expanding the charge eras by moving forward the light-absorbing surface range. In expansion, the well-formed arrange between inorganic InP QDs and natural P3HT:PC70BM dynamic layer were diminished RS and moved forward the portability, since it makes a difference charge exchange and charge collection. The frequency response of the detector without the scintillator was evaluated using a pulsed green LED (emission peak at 540 nm).

6 Conclusion and Future Perspectives

The combination of developed X-ray techniques and synthesis of X-ray activated scintillators have offered excellent technology in medical radiography, diagnosis, and deep-tumor therapy. The nanoscale scintillators serve as a contrast medium in low dosage CT imaging. Owing to the boundless infiltration profundity of X-ray, the comparing scintillator shows extraordinary potential for the focus on the treatment of profound situated tumors. The high X-ray attenuation coefficient reduces the possibility of destruction of healthy tissues and organs in radiotherapy. However, the new materials with optimization of X-ray activated nanoscintillator will always remain and very essential for the progress of radiographic and therapeutic facilities for the diagnosis and treatment of deep-tumor in clinical level. For this, work

in incredible collaborations and near co-operation between researchers, engineers, doctors, and drug specialists are direly required within the precise assessment of the treatment viability and side impacts of the intra-tumor infused scintillators, which is exceptionally vital for assist progressing the remedy rate of cancer and extraordinarily dragging out the life of the patients. We have to appreciate the work done and the efforts made so far which brought a lots of achievement and the possibility for the X-ray activated scintillators in biomedical scenario. However, the theoretical understanding to find the accurate band structures, and the mechanisms of charge and energy transfer, is on centered which need to be tackled before experiment that obviously helps to improve the photoluminescence (PL) performances and may open the broad applications.

Acknowledgements GN and SKS are very thankful to funding agencies CAPES, CNPq and FAPEMA, Brazil; SKS is also very thankful to PPGF-UFMA for motivation to work on this book project. JAHC thanks the CNPq and FAPDF, Brazil for the financial support. Dr. Mohan C. Mathpal greatly acknowledges the funding from FONDECYT program (N ° 3190316) to support the research activity. J.R.M and M.C. acknowledge the support from ANID Fondequip EQM140168.

References

1. Nikl M, Yoshikawa A (2015) Recent R&D trends in inorganic single-crystal scintillator materials for radiation detection. Adv Opt Mater 3:463–481. https://doi.org/10.1002/ADOM.201400571
2. De Jonge MD, Vogt S (2010) Hard X-ray fluorescence tomography-an emerging tool for structural visualization. Curr Opin Struct Biol 20:606–614
3. Xu L-J, Lin X, He Q, Worku M, Ma B (2020) Highly efficient eco-friendly X-ray scintillators based on an organic manganese halide. Nat Commun 111(11):1–7. https://doi.org/10.1038/s41467-020-18119-y
4. Wei H, Bruns OT, Kaul MG, Hansen EC, Barch M, Wiśniowska A, Chen O, Chen Y, Li N, Okada S, Cordero JM, Heine M, Farrar CT, Montana DM, Adam G, Ittrich H, Jasanoff A, Nielsen P, Bawendi MG (2017) Exceedingly small iron oxide nanoparticles as positive MRI contrast agents. Proc Natl Acad Sci USA 114:2325–2330. https://doi.org/10.1073/pnas.1620145114
5. James ML, Gambhir SS (2012) A molecular imaging primer: Modalities, imaging agents, and applications. Physiol Rev 92:897–965
6. Birowosuto MD, Cortecchia D, Drozdowski W, Brylew K, Lachmanski W, Bruno A (2016) Soci C (2016) X-ray Scintillation in Lead Halide Perovskite Crystals. Sci Reports 61(6):1–10. https://doi.org/10.1038/srep37254
7. Bertrand GHV, Hamel M, Sguerra F (2014) Current status on plastic scintillators modifications. Chem A Eur J 20:15660–15685. https://doi.org/10.1002/CHEM.201404093
8. Buck C, Yeh M (2016) Metal-loaded organic scintillators for neutrino physics. J Phys G Nucl Part Phys 43. https://doi.org/10.1088/0954-3899/43/9/093001
9. Kharzheev YN (2015) Scintillation counters in modern high-energy physics experiments (Review). Phys Part Nucl 464(46):678–728. https://doi.org/10.1134/S1063779615040048
10. Dujardin C, Auffray E, Bourret-Courchesne E, Dorenbos P, Lecoq P, Nikl M, Vasil'Ev AN, Yoshikawa A, Zhu RY (2018) Needs, trends, and advances in inorganic scintillators. IEEE Trans Nucl Sci 65:1977–1997. https://doi.org/10.1109/TNS.2018.2840160

11. Hsieh J (2009) Computed tomography principles, design, artifacts, and recent advances. SPIE, Bellingham, WA
12. Ketcham RA, Carlson WD (2001) Acquisition, optimization and interpretation of x-ray computed tomographic imagery: applications to the geosciences. Comput Geosci 27:381–400. https://doi.org/10.1016/S0098-3004(00)00116-3
13. Grassler T, Wirth KE (2000) X-ray computer tomography-potential and limitation for the measurement of local solids distribution in circulating fluidized beds. Chem Eng J 77:65–72. https://doi.org/10.1016/S1385-8947(99)00133-3
14. The Fundamentals of X-ray and radium physicsthe fundamentals of X-ray and radium physics (1954) By SelmanJoseph, M.D., Director, School for X-ray Technicians, Tyler Junior College; Chief of Radiology, Mother Frances Hospital; Director, Radiology Department, Medical Center Hospital; Consultant in Radiology, East Texas Tuberculosis Hospital, Tyler, Texas. A volume of 340 pages, with 174 illustrations and 8 tables. Published by Charles C Thomas, Springfield, Ill.1954 Price $8.50 Radiology 63:264–265. https://doi.org/10.1148/63.2.264b
15. Cartz L (1995) Nondestructive testing. ASM International, Material Park, OH
16. Kudryashov YB (2008) Radiation biophysics ionizing radiations. Nova Science Pub Inc
17. Kherlopian AR, Song T, Duan Q, Neimark MA, Po MJ, Gohagan JK, Laine AF (2008) A review of imaging techniques for systems biology. BMC Syst Biol 2
18. Chotas HG, Dobbins JT, Ravin CE (1999) Principles of digital radiography with large-area, electronically readable detectors: a review of the basics. Radiology 210:595–599
19. Seeger A, Kertzscher U, Affeld K, Wellnhofer E (2003) Measurement of the local velocity of the solid phase and the local solid hold-up in a three-phase flow by X-ray based particle tracking velocimetry (XPTV). Chem Eng Sci 58:1721–1729. https://doi.org/10.1016/S0009-2509(03)00010-1
20. Heindel TJ, Gray JN, Jensen TC (2008) An X-ray system for visualizing fluid flows. Flow Meas Instrum 19:67–78. https://doi.org/10.1016/j.flowmeasinst.2007.09.003
21. Johnson Q, Pellinen D (1979) Flash X-ray. Sagamore Army Mater Res Conf Proc 117–150. https://doi.org/10.1007/978-1-4613-2952-7_6
22. Jamet F, Thomer G (1976) Flash radiography 192
23. Heindel TJ (2011) A review of X-ray flow visualization with applications to multiphase flows. J Fluids Eng Trans ASME 133. https://doi.org/10.1115/1.4004367/456290
24. Shalom NE, Gong GX, Auster M (2020) Fluoroscopy: an essential diagnostic modality in the age of high-resolution cross-sectional imaging. World J Radiol 12:213. https://doi.org/10.4329/WJR.V12.I10.213
25. Covello B, McKeon B (2022) Fluoroscopic angiography assessment, protocols, and interpretation. StatPearls Publishing
26. McRae R, Bagchi P, Sumalekshmy S, Fahrni CJ (2009) In situ imaging of metals in cells and tissues. Chem Rev 109:4780–4827. https://doi.org/10.1021/cr900223a
27. Fahrni CJ (2007) Biological applications of X-ray fluorescence microscopy: exploring the subcellular topography and speciation of transition metals. Curr Opin Chem Biol 11:121–127
28. Shimura M, Saito A, Matsuyama S, Sakuma T, Terui Y, Ueno K, Yumoto H, Yamauchi K, Yamamura K, Mimura H, Sano Y, Yabashi M, Tamasaku K, Nishio K, Nishino Y, Endo K, Hatake K, Mori Y, Ishizaka Y, Ishikawa T (2005) Element array by scanning X-ray fluorescence microscopy after cis-diamminedichloro-platinum(II) treatment. Cancer Res 65:4998–5002. https://doi.org/10.1158/0008-5472.CAN-05-0373
29. Ortega R, Devès G, Carmona A (2009) Bio-metals imaging and speciation in cells using proton and synchrotron radiation X-ray microspectroscopy. J Royal Soc Interface Royal Soc 6: S469-S658
30. Miqueles EX, De Pierro AR (2010) Exact analytic reconstruction in x-ray fluorescence CT and approximated versions. Phys Med Biol 55:1007–1024. https://doi.org/10.1088/0031-9155/55/4/007
31. Marmorato P, Ceccone G, Gianoncelli A, Pascolo L, Ponti J, Rossi F, Salomé M, Kaulich B, Kiskinova M (2011) Cellular distribution and degradation of cobalt ferrite nanoparticles in Balb/3T3 mouse fibroblasts. Toxicol Lett 207:128–136. https://doi.org/10.1016/j.toxlet.2011.08.026

32. Milakovic M, Berg G, Eggertsen R, Nyström E, Olsson A, Larsson A, Hansson M (2006) Determination of intrathyroidal iodine by X-ray fluorescence analysis in 60 to 65 year olds living in an iodine-sufficient area. J Intern Med 260:69–75. https://doi.org/10.1111/j.1365-2796.2006.01660.x
33. Studinski R, O'Meara J, McNeill F (2008) The feasibility of in vivo measurement of arsenic and silver by x-ray fluorescence. X-ray Spectrom 37:51–57. https://doi.org/10.1002/xrs.1010
34. Hoppin JA, Aro ACA, Williams PL, Hu H, Ryan PB (1995) Validation of K-XRF bone lead measurement in young adults. Environ Health Perspect 103:78–83. https://doi.org/10.1289/ehp.9510378
35. Mach JC, Omar A, Barone HE, Harb A, Abujudeh H (2021) Fluoroscopy and MRI induced skin injuries: a review of diagnostic, management, and preventative principles. Curr Radiol Reports 91(9):1–10. https://doi.org/10.1007/S40134-020-00376-W
36. Green JD, Omary RA, Schirf BE, Tang R, Lu B, Gehl JA, Huang JJ, Carr JC, Pereles FS, Li D (2005) Comparison of X-ray fluoroscopy and interventional mri for the assessment of coronary artery stenoses in swine. Magn Reson Med 54:1094. https://doi.org/10.1002/MRM.20699
37. Wang J, Blackburn TJ (2000) The AAPM/RSNA physics tutorial for residents. 20:1471–1477. https://doi.org/10.1148/radiographics.20.5.g00se181471
38. Seeram E (2019) Digital Fluoroscopy. Digit Radiogr 95–110. https://doi.org/10.1007/978-981-13-3244-9_6
39. Graham MT, Assis F, Allman D, Wiacek A, Gonzalez E, Gubbi MR, Dong J, Hou H, Beck S, Chrispin J, Bell MAL (2020) Photoacoustic image guidance and robotic visual servoing to mitigate fluoroscopy during cardiac catheter interventions. 11229:80–85. https://doi.org/10.1117/12.2546910
40. Yang Y, Tian Q, Wang D, Yi F, Song H, Li W, Wu C (2021) Percutaneous vertebroplasty for C1 osteolytic lesions via lateral approach under fluoroscopic guidance . J Pain Res 14:2121–2128. https://doi.org/10.2147/JPR.S318236
41. Huang SY, Damasco JA, Tian L, Lu L, Perez JVD, Dixon KA, Williams ML, Jacobsen MC, Dria SJ, Eggers MD, Melancon AD, Layman RR, Whitley EM, Melancon MP (2020) In vivo performance of gold nanoparticle-loaded absorbable inferior vena cava filters in a swine model. Biomater Sci 8:3966–3978. https://doi.org/10.1039/D0BM00414F
42. Bohari A, Hashim S, Mohd Mustafa SN (2020) Scatter radiation in the fluoroscopy-guided interventional room. Radiat Prot Dosimetry 188:397–402. https://doi.org/10.1093/RPD/NCZ299
43. Kimura M, Castillo M (2013) Basic principles of computed tomography angiography (CTA). Vasc Imaging Cent Nerv Syst Phys Princ Clin Appl Emerg Tech 67–82. https://doi.org/10.1002/9781118434550.CH4
44. Ivancevic MK, Geerts L, Weadock WJ, Chenevert TL (2009) Technical principles of MR angiography methods. Magn Reson Imaging Clin N Am 17:1–11. https://doi.org/10.1016/J.MRIC.2009.01.012
45. Htyte N, Jenkins JS (2014) Diagnostic cerebral and peripheral angiography. Pan Vascular Med 1–55. https://doi.org/10.1007/978-3-642-37393-0_39-1
46. Ishihara S, Ross IB, Piotin M, Weill A, Aerts H, Moret J (2000) 3D rotational angiography: recent experience in the evaluation of cerebral aneurysms for treatment. Interv Neuroradiol 6:85. https://doi.org/10.1177/159101990000600202
47. Van Rooij WJ, Sprengers ME, De Gast AN, Peluso JPP, Sluzewski M (2008) 3D rotational angiography: the new gold standard in the detection of additional intracranial aneurysms. AJNR Am J Neuroradiol 29:976–979. https://doi.org/10.3174/AJNR.A0964
48. Kaplan DJ, Patel JN, Liporace FA, Yoon RS (2016) Intraoperative radiation safety in orthopaedics: a review of the ALARA (As low as reasonably achievable) principle. Patient Saf Surg 101(10):1–7. https://doi.org/10.1186/S13037-016-0115-8
49. Nimi N, Saraswathy A, Nazeer SS, Francis N, Shenoy SJ, Jayasree RS (2018) Biosafety of citrate coated zerovalent iron nanoparticles for magnetic resonance angiography. Data Br 20:1829–1835. https://doi.org/10.1016/J.DIB.2018.08.157

50. Islam K, Haque M, Kumar A, Hoq A, Hyder F, Hoque SM (2020) Manganese Ferrite Nanoparticles ($MnFe_2O_4$): size dependence for hyperthermia and negative/positive contrast enhancement in MRI. Nanomater 10:2297. https://doi.org/10.3390/NANO10112297
51. Tavakol M, Ashraf S, Brener SJ (2012) Risks and complications of coronary angiography: a comprehensive review. Glob J Health Sci 4:65. https://doi.org/10.5539/GJHS.V4N1P65
52. Withers PJ, Bouman C, Carmignato S, Cnudde V, Grimaldi D, Hagen CK, Maire E, Manley M, Du Plessis A (2021) Stock SR (2021) X-ray computed tomography. Nat Rev Methods Prim 11(1):1–21. https://doi.org/10.1038/s43586-021-00015-4
53. Garvey CJ, Hanlon R (2002) Computed tomography in clinical practice. BMJ Br Med J 324:1077. https://doi.org/10.1136/BMJ.324.7345.1077
54. Bockisch A, Freudenberg LS, Schmidt D, Kuwert T (2009) Hybrid imaging by SPECT/CT and PET/CT: proven outcomes in cancer imaging. Semin Nucl Med 39:276–289. https://doi.org/10.1053/J.SEMNUCLMED.2009.03.003
55. Ter-Pogossian MM (1977) Basic principles of computed axial tomography. Semin Nucl Med 7:109–127. https://doi.org/10.1016/S0001-2998(77)80013-5
56. Seeram E (2010) Computed tomography: physical principles and recent technical advances. J Med Imaging Radiat Sci 41:87–109. https://doi.org/10.1016/J.JMIR.2010.04.001
57. Novelline RA, Rhea JT, Rao PM, Stuk JL (1999) Helical CT in emergency radiology. Radiology 213:321–339. https://doi.org/10.1148/RADIOLOGY.213.2.R99NV01321
58. Silverman PM, Cooper CJ, Weltman DI, Zeman RK (1995) Helical CT: practical considerations and potential pitfalls. Radiographics 15:25–36. https://doi.org/10.1148/RADIOGRAPHICS.15.1.7899611
59. Sun ZH, Cao Y, Li HF (2011) Multislice computed tomography angiography in the diagnosis of coronary artery disease. J Geriatr Cardiol 8:104. https://doi.org/10.3724/SP.J.1263.2011.00104
60. Goldman LW (2008) Principles of CT: multislice CT. J Nucl Med Technol 36:57–68. https://doi.org/10.2967/JNMT.107.044826
61. Tawfik HA, Abdelhalim A, Elkafrawy MH (2012) Computed tomography of the orbit - A review and an update. Saudi J Ophthalmol Off J Saudi Ophthalmol Soc 26:409–418. https://doi.org/10.1016/J.SJOPT.2012.07.004
62. Xue N, Zhou C, Chu Z, Chen L, Jia N (2020) Barley leaves mediated biosynthesis of Au nanomaterials as a potential contrast agent for computed tomography imaging. Sci China Technol Sci 642(64):433–440. https://doi.org/10.1007/S11431-019-1546-3
63. Dong YC, Hajfathalian M, Maidment PSN, Hsu JC, Naha PC, Si-Mohamed S, Breuilly M, Kim J, Chhour P, Douek P, Litt HI, Cormode DP (2019) Effect of gold nanoparticle size on their properties as contrast agents for computed tomography. Sci Reports 91(9):1–13. https://doi.org/10.1038/s41598-019-50332-8
64. Fayngersh V, Passero M (2009)Estimating radiation risk from computed tomography scanningLung 187:143–148. https://doi.org/10.1007/S00408-009-9143-9
65. Cui Y, Zhang J, He H, Qian G (2018) Photonic functional metal–organic frameworks. Chem Soc Rev 47:5740–5785. https://doi.org/10.1039/C7CS00879A
66. Wei H, Huang J (2019) Halide lead perovskites for ionizing radiation detection. Nat Commun 101(10):1–12. https://doi.org/10.1038/s41467-019-08981-w
67. Nikl M (2016) Nanocomposite, ceramic, and thin film scintillators, 1st edn. Jenny Standard Publishing
68. Wang Y, Yin X, Chen J, Wang Y, Chai Z, Wang S (2020) Gleaming uranium: an emerging emitter for building X-ray scintillators. Chem A Eur J 26:1900–1905. https://doi.org/10.1002/CHEM.201904409
69. Wei Y, Cheng Z, Lin J (2019) An overview on enhancing the stability of lead halide perovskite quantum dots and their applications in phosphor-converted LEDs. Chem Soc Rev 48:310–350. https://doi.org/10.1039/C8CS00740C
70. Zhu H, Zhang P, Dai S (2015) Recent advances of lanthanum-based perovskite oxides for catalysis. ACS Catal 5:6370–6385. https://doi.org/10.1021/ACSCATAL.5B01667